Modeling of Sintering and Redispersion of Supported Metal Catalysts

A model, which utilizes a Monte Carlo simulation, of the sintering and the redispersion of supported metal catalysts is presented and compared with experimental data from a Pt/Al_2O_3 system. The model is based on an atomic migration mechanism, but includes instantaneous diffusion and coalescence of crystallites of size <1 nm in reducing and inert atmospheres. It was found that behavior in reducing, oxidizing and inert atmospheres could be predicted.

P. K. HANDA
and J. C. MATTHEWS

Department of Chemical Engineering
Kansas State University
Manhattan, KS 66506

SCOPE

Supported metal catalysts are used extensively in the process industry. An early application was the reforming of naptha to high-octane gasoline using Pt on an alumina support. Most hydrogenations are done with either Ni or Pd on a suitable support. Presently, Pt along with other metals is used in the catalytic mufflers of automotive exhausts. The support makes it possible for a high percentage of the metal atoms to be exposed, thus making efficient utilization of the metal.

One of the problems of supported metal catalysts is sintering, that is a decrease in metal surface area due to the growth or agglomeration of crystallites, which occurs at elevated temperatures. Several processes, among them treatment with oxygen and chlorine, have been found to achieve redispersion of the metal on the support. Obviously *in situ* redispersion is of considerable industrial importance as it prolongs the life of the catalyst.

Fundamental studies of the processes occuring during sintering and redispersion are valuable in designing new catalysts and in reducing sintering in existing processes. Two major concepts have been employed to model the sintering and redispersion of supported metal catalysts, namely, sintering by particle migration (Ruckenstein and Pulvermacher, 1973a,b) and sintering by atomic migration (Flynn and Wanke, 1974a). A study of the sintering and redispersion of supported metal catalysts, based on the atomic migration concept proposed by Flynn and Wanke (1974b), has been made in this work. The model uses escape of atoms to the support, diffusion on the surface and collision with the crystallites. A Monte Carlo method of solution was employed.

Experimental results for the Pt/Al_2O_3 system have been compared with model predictions. Changes in crystallite size and dispersion have been measured by H_2 chemisorption in a static, volumetric BET apparatus.

CONCLUSION AND SIGNIFICANCE

Pt crystallites on Al_2O_3 were subjected to alternate treatments in H_2 and O_2 for various times and temperatures. It was found that sintering which occurred in H_2 could be redispersed by treatment in oxygen. However, no redispersion of crystallites sintered in oxygen was obtained.

A model of the phenomena was developed which viewed the behavior of hydrogen sintered catalyst when subjected to O_2 as resulting from a very rapid loss of Pt from the crystallites to the support surface followed by slow transport on the surface and a low probability of incorporation into a crystallite upon collision. The behavior in H_2 and in He was described by very rapid transport on the support surface, no resistance to capture but very slow loss of Pt from the crystallites. Using this model it was possible to predict the changes in dispersion that occur during sequences involving alternate treatments in H_2 and O_2.

The state of the metal in an O_2 atmosphere was described differently than in an H_2 or He atmosphere. For 100% dispersion in H_2, the metal was assumed to be present as 1 nm crystallites while in O_2 the metal was assumed to be spread over the surface of the support, probably as an oxide, though treated as free atoms. Nucleation in O_2 took place at specific sites on the support, and sintering occurred as the crystallites grew at these sites. If this partially O_2 sintered catalyst was subjected to H_2, the remaining free atoms were assumed to immediately coalesce into 1-nm crystallites and the sintering proceeded with these crystallites and those previously formed in O_2.

While the state of the metal in an O_2 atmosphere is described as free atoms, this aspect of the model is intended to be largely consistent with the dispersed-phase description (Yao et al., 1979) and with the two-dimensional fluid description (Ruckenstein and Chu, 1979).

Several simulations showed that either sintering or redispersion could be predicted depending on the initial particle-size distribution for the same dispersion. One simulation, done at two levels of dispersion (0.55 and 0.41), predicted that if these two catalysts were examined after the same elapsed time, one (0.55) would exhibit sintering while the other would exhibit redispersion.

BACKGROUND

Sintering of metal crystallites is one of the primary causes of deactivation. With Pt, Ir, etc. various processes (Kearby et al., 1964; Coe et al., 1965; Brennan et al., 1964; Webb, 1961; and Malo et al., 1959) for reactivation have been found which include a redispersion of the metal on the support. Much of this early work deduces redispersion because of restoration of activity. More recently, several references (Maat et al., 1975; Ruckenstein et al., 1976; Baker et al., 1975; Chen et al., 1978; Ruckenstein et al., 1979; McVicker

Correspondence concerning this paper should be addressed to John Matthews.

et al., 1978; and Wang et al., 1980) have reported a decrease in crystallite size as measured by electron microscopy.

Dautzenberg and Wolters (1978) found that heat treatment in H_2 (773–948 K) of Pt/Al_2O_3 resulted in decreased H_2 chemisorption but no change in crystallite size and no redispersion on subjection to O_2. Either sintering or restoration of Pt rendered "inaccessible" by previous maltreatment in H_2 was observed. den Otter and Dautzenberg (1978) reported that the inaccessible Pt was the result of the Pt alloying with the Al of the Al_2O_3 support. Menon and Froment (1979) and Yao et al. (1979) disputed this interpretation. For Pt/TiO_2 system, Baker et al. (1979a, 1979b) observed a strong interaction between metal and support in an H_2 environment which can be destroyed by a subsequent oxidative treatment. Nothing similar to this was observed for Pt/Al_2O_3.

Ruckenstein and Chu (1979) found that, for Pt crystallites supported on a nonporous alumina film, after several H_2 and O_2 cycles at 1,023 K sintering occurred during reduction and redispersion during oxidation. They suggested that redispersion is caused either by the fracture of the crystallites or by spreading of platinum oxide over the substrate surface. Based on his experimental results on Pt/TiO_2, Baker (1980) supported the concept of sintering and redispersion being functions of wetting angle, as suggested by Ruckenstein and Chu (1979). Yao et al. (1979) proposed that redispersion of Pt supported on alumina can be understood by the formation of a two-dimensional phase which covers ~10% of the surface of the support at saturation, but which exists only at temperatures where platinum oxide is stable. Thus, when a Pt/Al_2O_3 catalyst is heated under reducing conditions or in an oxygen-containing environment but at temperatures above the decomposition temperature of platinum oxide, the platinum will be primarily in the metallic state and any individual platinum atoms will quickly agglomerate into particles. If the same catalyst is then treated in O_2 at 773 K, some platinum oxide will form and lead to redispersion. In the presence of excess platinum, a bulk oxide is also present, and some surface area loss could continue to be observed after redispersion as a result of the coarsening of the bulk phase.

Stulga et al. (1980) observed no significant change in platinum particle size for initially heat-treated samples which were subsequently "redispersed" in air at 773 K for 18 hours. These results are in contradiction to the observations made by Ruckenstein and Malhotra (1976) who found a decrease in Pt particle size, from 10.7 to 7.1 nm under similar heat treatment conditions. Straguzzi et al. (1980) found that hydrogen-sintered, but not air-sintered, Pt/Al_2O_3 catalysts could be easily redispersed by air treatment at 773 K. However, the air-sintered catalysts were redispersed by O_2 treatment at 773 K. Wang and Schmidt (1980) studied the effects of air and hydrogen treatments on 2–10 nm diameter particles of Ir on amorphous SiO_2. Gradual heating of the samples in air resulted in formation of Ir oxide around the metal particles and the spreading of this Ir oxide in a thin layer over the SiO_2. At 1,023 K the residual metal particles broke into clusters of several 1–3 nm particles. Subsequent heating in H_2 at 673 K reduced the oxide and clusters of small Ir particles were formed. These remained stable to ~873 K, above which sintering to larger particles occurred.

Two mathematical models based on different mechanisms for sintering and redispersion have been proposed. The "crystallite migration model" developed by Ruckenstein and Pulvermacher (1973a, 1973b) envisages the sintering to occur by migration of metal crystallites over the support surface, and the resulting collision and fusion of metal particles causes the loss of dispersion. The "atomic migration model" proposed by Flynn and Wanke (1974a) considered the sintering to occur by dissociation of atomic or molecular species from the metal crystallites. These atomic or molecular species migrate over the support surface and become incorporated into the metal crystallites upon collision with the stationary crystallites. A detailed comparison of the two models has been presented by Wanke and Flynn (1975).

Ruckenstein and Dadyburjor (1977) proposed a model which combines the characteristics of both the atomic and the crystalline migration models. Wynblatt et al. (1976) proposed that particle growth can occur in either a "noninhibited" or an "inhibited" mode. In inhibited particle growth, faceting of the metal crystallites slows growth by requiring a nucleation process for each new layer of atoms added to the particle. Lee (1980) showed that the rate of loss of metal surface area is not simply proportional to a power of the metal area if atomic migration is the mechanism.

Controlled atmosphere electron microscopy experiments using model Pt/Al_2O_3 (Baker et al., 1975), Pt/SiO_2 (Chen and Schmidt, 1978), Ir/Al_2O_3 (McVicker et al., 1978), and Ir/SiO_2 (Wang and Schmidt, 1980) catalysts seem to favor the atomic migration mechanism.

DESCRIPTION OF THE MODEL

The sintering and redispersion process was modelled as loss of atomic or molecular species by metal crystallites to the support, migration of these species over the support surface, and their incorporation into the metal crystallites. The model is highly idealized and was solved by the Monte Carlo technique. This technique permits the study of nucleation of completely dispersed metal which frequently occurs. The technique also allows the study of sintering when all crystallites have the same size and when the crystallites are not randomly dispersed on the support.

Loss of Atoms or Molecular Species from Crystallites

It has been argued that since the interaction of metals with the nonmetallic surfaces of support is small, dissociation of atoms to the support surface is not very likely at moderate temperatures due to the large activation energy requirements. Flynn and Wanke (1974) presented qualitative arguments that strong metal-support interactions could lower this activation energy. Also the formation of volatile compounds in the presence of reactive gases and their desorption from crystallites to the gas phase cannot be discounted. For example, using the experimental vapor pressure data for bulk platinum (Dreger and Margrave, 1960), the equilibrium data for platinum-oxygen (Schafer and Tebben, 1960), the vapor pressure of Pt and PtO_2 as a function of particle radius was calculated utilizing the Kelvin equation. The maximum evaporation rates were then computed (de Boer, 1968). For a 4-nm crystallite in oxygen at 50.65 kPa and 823 K, the evaporation rate of PtO_2 is 12 atoms/s compared to 1×10^{-16} atom/s for Pt in an inert atmosphere.

The fraction, Φ, of metal surface atoms lost from a crystallite to the support as a function of crystallite size was needed. The Kelvin equation predicts that smaller crystallites have a greater vapor pressure than larger crystallites. A part of the increased vapor pressure may be attributed to the decreased number of bonds between atoms in the smaller crystallite. A decrease in coordination number is a measure of this decrease and in this work an average coordination number, SCN, for the surface atoms of a crystallite was first calculated.

$$SCN = \frac{1}{N_S}\left[(N_{\text{corner}})(CN)_{\text{corner}} + (N_{\text{edge}})(CN)_{\text{edge}} + (N_{\text{face}})(CN)_{\text{face}}\right] \quad (1)$$

The maximum value of SCN for an FCC structure is 8 and corresponds to an infinitely large crystallite with no edge or corner atoms. For a 5-nm crystallite, $N_{\text{corner}} = 8$, $N_{\text{edge}} = 103$ and $N_{\text{face}} = 993$ resulting in an SCN of 7.691. Any departure of SCN from 8 was viewed as an increasing tendency to evaporate and Φ for any crystallite of size greater than 1 nm was modelled as $(8 - SCN)/8$. It was assumed that all atoms of crystallites less than 1 nm in size escape to the support.

After the fraction Φ of metal atoms were transferred to the support surface, the remaining atoms of the crystallite were rearranged so that the original shape was retained.

The equations of Hardeveld and Hartog (1969) for FCC cubes were used to determine the number of surface, total and bulk atoms of the crystallites.

$$N_S = (12\ \text{m}^2 - 24\ \text{m} + 14)/1.2 \quad (2)$$

$$N_T = 4\ \text{m}^3 - 6\ \text{m}^2 - 3\ \text{m} \quad (3)$$

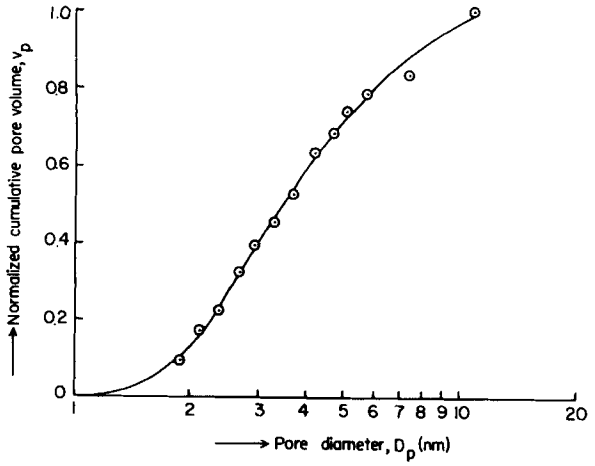

Figure 1. Normalized cumulative pore volume vs. pore diameter for Kaiser 201 alumina.

$$N_B = N_T - N_S \tag{4}$$

In Eq. 2, a factor of 1.2 was introduced to achieve agreement between these calculations and the particle size calculations from the chemisorption results. To translate dispersion, measured by chemisorption into average crystallite size, it was assumed that all particles were ideal cubes with one face in contact with the support and the remaining five faces exposed. Thus one out of every 1.2 surface atoms was assumed to be accessible for hydrogen chemisorption.

The simulation was two dimensional and for purposes of ascertaining collision between a diffusing atom and a crystallite, the simulated crystallite was assumed to be circular. The diameter of the circle was taken to be the diameter of a sphere having the same volume as that of the cube determined from chemisorption. Equating volumes and utilizing the FCC structures yields

$$m = 1 + \frac{0.806D - d_o}{\sqrt{2}d_o} \tag{5}$$

Migration of Atoms or Molecular Species over Support Surface

The migration of atoms over the support surface was viewed as hopping from one location on the support to another. The number of times an atom hops is the number of diffusion steps and is a function of temperature, atmosphere and metal-support system. Step length determined from the experimentally measured pore-size distribution of the support (Kaiser 201 alumina) was used. Normalized cumulative pore volume vs. pore diameter for the alumina, measured by nitrogen adsorption, is shown in Figure 1 (macropores of size >11 nm, not included). To assign a value to the step length a random number, R_1, in the interval (0,1) was selected and equated to V_p. From Figure 1, the value of D_p corresponding to the above value of V_p was used as the step length.

Collision and Capture of Atoms or Molecular Species by Metal Crystallites

On collision with a metal crystallite, the atom may become incorporated into the crystallite depending on the sticking probability associated with the crystallite. Howard et al. (1967), Hansen (1976), and Bonzel et al. (1973) have reported values of sticking probabilities varying from 0.02 to >0.9 for various gas-metal systems. In H_2 and in inert atmospheres, no barriers to capture were believed to exist and the sticking probability was set equal to unity. Where capture was believed to be more difficult, as in oxygen, in the absence of other data a sticking probability of $1 - \Phi$ was used. Capture sites seem to be shielded in oxygen in a manner that does not exist in H_2 or He atmospheres.

TABLE 1. CRYSTALLITE-SIZE DISTRIBUTION USED IN THIS STUDY

			PSD	
N Total Atoms	Dispersion	Distribution Designation	D_i, nm Diameter	n_i Number with Diameter D_i
55,000	0.55	σ20	1.725	367
55,000	0.55	σ2m	3.778	20
			1.0	778
55,000	0.55	BP1	9.413	1
			1.0	1,031
55,000	0.41	σ20	2.5	114
55,000	0.41	σ2m	6.643	4
			1.0	611
55,000	0.41	BP1	10.267	1
			1.0	706

MONTE CARLO SIMULATION

The Monte Carlo simulation requires that support dimensions, crystallite size distribution, and evaporation-diffusion mechanism be known.

The model is two-dimensional and the support was assumed to be square. The mass of the support can be determined from the metal loading and the number of metal atoms to be considered in the simulation. The area of the support can then be obtained from the specific surface area and a side of the square can thus be calculated.

$$D_s = \left(S_s \cdot \frac{100}{L} \cdot \frac{MW_m}{A} \cdot N\right)^{1/2} \tag{6}$$

The number of atoms used in the simulation was 55,000. This value gave what were considered to be reasonable numbers of crystallites. For the case of 1.62% Pt on Al_2O_3 having a specific surface area of 300 m^2/g, D_s was found to be 574.4 nm.

It was suspected that the simulation could be scaled by assuming that the ratio of support-side lengths would equal the square root of the ratio of the number of diffusion steps. This assumption, the accuracy of which was tested for four different initial dispersions, was found to be excellent and was used throughout the work. For example, a support of 574.4 nm and 660 diffusion steps could be replaced by a 100-nm support and 20 diffusion steps.

Crystallite Size Distributions

Three crystallite-size distributions, for a given initial dispersion and total number of atoms in the system, were generated. One distribution, σ20, had all crystallites of the same size and thus a minimum variance. Another, σ2m, was constructed such that it was bidisperse with the smaller size set at 1 nm. The size of the larger crystallites and the number of crystallites of each size were determined such that the variance of this distribution was a maximum. The third distribution, BP1, consisted of one large crystallite and the remainder 1-nm crystallites. A fourth distribution, a skewed Gaussian with a large fraction of small crystallites, was also investigated (Handa, 1981) but not reported here. The distributions are listed in Table 1.

Evaporation-Diffusion Mechanism

Three different combinations of evaporation and diffusion rates were considered. The first corresponded to rapid evaporation from the crystallite and slow diffusion of the atoms. For this case, it was assumed that the atoms which evaporated from the crystallite did so at $t = 0$. The diffusion and collision processes were then monitored. The flow of time in this case is represented by the number of diffusion steps. The extent of evaporation was varied by an adjustable parameter, ϵ, which multiplies Φ and which would be expected to vary with temperature, atmosphere and metal-support system.

The rate of evaporation was controlling in the second case and was modelled as atoms evaporating at a finite rate and instantaneously being captured by crystallites. The finite range of evaporation was achieved by letting the evaporation occur in a series of discrete steps. An increasing number of evaporation steps corresponds to increasing time in this case.

The third case corresponded to comparable rates of evaporation and diffusion.

Implementation of Monte Carlo Simulation

The computational scheme consisted of the following steps.

1. Crystallites were randomly distributed on the support.
2. The number of atoms evaporating from the crystallites at time zero was selected.
3. A new crystallite size distribution based on the number of atoms remaining on each crystallite was calculated.
4. The collision diameter, which was taken as the arithmetic average of the original and the new diameter, was calculated.
5. The number of atoms, I, to be monitored was selected.
6. Each atom was given a random initial location on the surface and the trajectory determined by determining the step length and a random angle. One atom at a time was monitored. If collision with a crystallite occurred a random number between 0 and 1 was generated. If this number was less than the sticking probability associated with the crystallite, the colliding atom was incorporated into the crystallite, otherwise the atom was allowed to take another random step.
7. For the instantaneous evaporation case the atoms were monitored until they had taken a given number of steps or were incorporated into a crystallite, whichever came first. Thus after I atoms had been monitored the number remaining on the support and the number colliding with each crystallite was known. This information was used to calculate a new crystallite size distribution and dispersion value.

For the instantaneous diffusion case the atoms were monitored until they were incorporated into a crystallite. A new crystallite size distribution was calculated based on the total atoms that evaporated and it was as if the atoms left a crystallite and were immediately assigned to either a new or the same crystallite.

For the comparable evaporation–diffusion case, I atoms were monitored for one step and a new crystallite size distribution and dispersion determined. Another evaporation then occurred and again I atoms were monitored. Among the I atoms were those from the first step that were not incorporated into a crystallite. These atoms continued from their previous position.

I was chosen to be 1,500 for the majority of this work. This number was selected after finding no significant change for selected cases when more atoms (up to 4,000) were monitored.

MODEL STUDIES

Before undertaking the simulation of the experimental results, some parameter studies were made. Unless otherwise specified, the calculations were performed with 55,000 total atoms and a metal loading of 1.62% on the Kaiser 201 alumina. The crystallite-size-dependent sticking probability was used and ϵ was set at 0.0045.

Effect of Particle-Size Distribution

Figures 2 and 3 show the effect of *PSD* for the case of instantaneous evaporation at two levels of dispersion. Figure 2 indicates that if the *PSD* is σ20, redispersion will be observed after an evaporation for the time period studied, while sintering will be observed for both σ2m and BPI. The difference may be attributed to the effects of the large crystallites present in σ2m and BPI. Relatively fewer atoms evaporate from the larger crystallites and the decrease in size and increase in dispersion with an evaporation is less significant than for smaller crystallites.

Comparing Figures 2 and 3 for σ20 indicates that at the higher

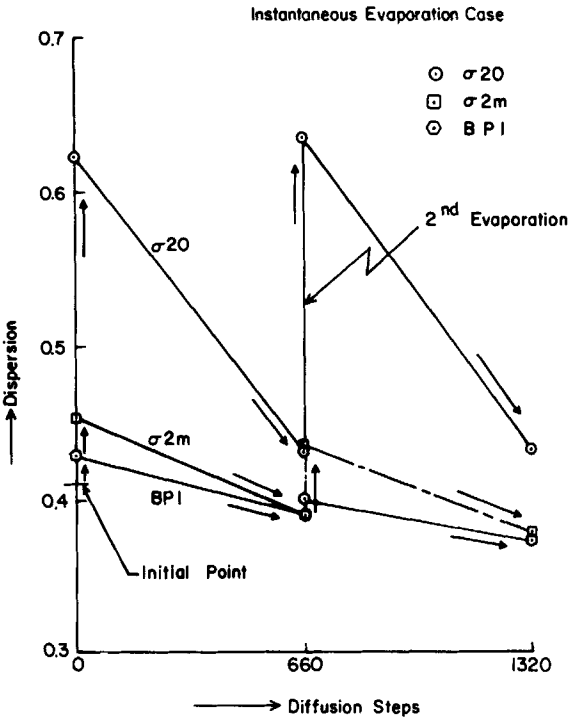

Figure 2. Effect of initial particle-size distribution on sintering rate (initial dispersion = 0.41).

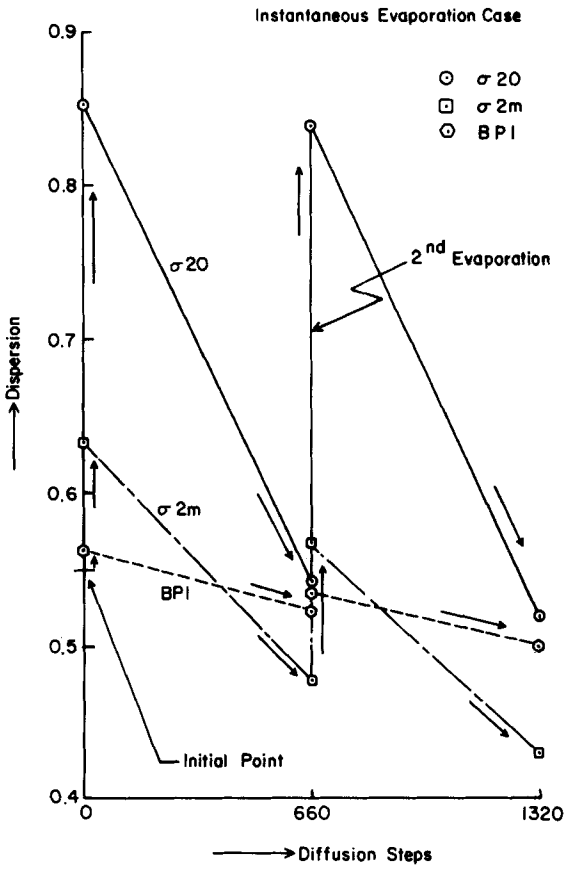

Figure 3. Effect of initial particle-size distribution on sintering rate (initial dispersion = 0.55).

dispersion level of Figures 3 sintering would be observed at the same time as redispersion was observed in Figure 2. Apparently the increased number of crystallites at the higher dispersion level has more than offset the decreased size. A similar effect explains the increased rate of sintering of σ2m relative to BPI with in-

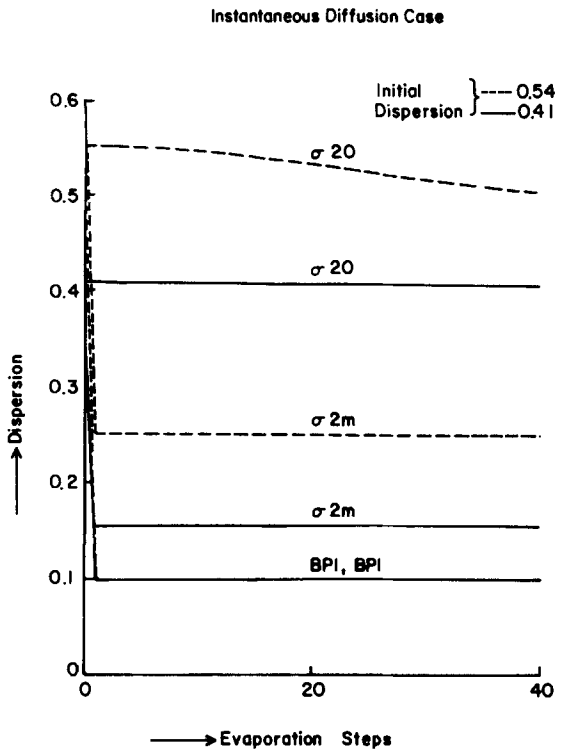

Figure 4. Effect of initial particle-size distribution on sintering rate (instantaneous diffusion mechanism).

creasing dispersion level as shown on Figures 2 and 3. Similar behavior was found for two levels of dispersion for the case of comparable evaporation-diffusion (Handa, 1981).

The instantaneous diffusion case is shown in Figure 4. For σ2m, the 1-nm crystallites are eliminated at the first evaporation. The slow sintering that follows is the result of the changes which occur in the unisized *PSD*, Figure 5. It is clear that the distribution broadens with time and particles of sizes smaller and larger than the originals appear. As time proceeds, the smaller particles disappear resulting in fewer but larger particles in the system. For PB1 the dispersion has fallen quickly to that of the large particle and remains constant as the atoms evaporate off but are immediately recaptured.

Effect of Evaporation Rate

Figure 6 shows the influence of variations in evaporation rate on sintering behavior. Higher evaporation rates result in more redispersion because of the larger number of free metal atoms on the support. When instantaneous diffusion is the governing mechanism (no free atoms present on the support surface), higher evaporation rates result in more sintering because, for higher evaporation rates, smaller crystallites appear on the larger ones. It was concluded that depending on the evaporation-diffusion mechanism, higher evaporation rates may result in either more redispersion or more sintering at a given time.

Effect of Location of Crystallite and Atoms

A brief examination of different combinations of crystallite and atom locations was made. This study was performed by locating the crystallites randomly but only on quadrants I and II of the square support surface. Calculations were then made in two ways. One was to assume that the initial location of the atoms to be monitored was random over the entire support. This should correspond to the case of extensive vapor-phase transport upon evaporation. The second method of calculation was to assume that the initial location of the atoms was in the vicinity of the crystallites and thus only in quadrants I and II.

The results for the comparable evaporation-diffusion mechanism and σ20 PSD are shown in Figure 7. They show that if atom location is independent of crystallite location, redispersion would be significantly enhanced and sintering postponed by deliberately locating the metal over only a portion of the support.

EXPERIMENTAL

Most of the redispersion work in oxygen environments has been restricted to 673–873 K. This has been explained by associating redispersion with a metal-support complex that is formed in the presence of oxygen. The upper

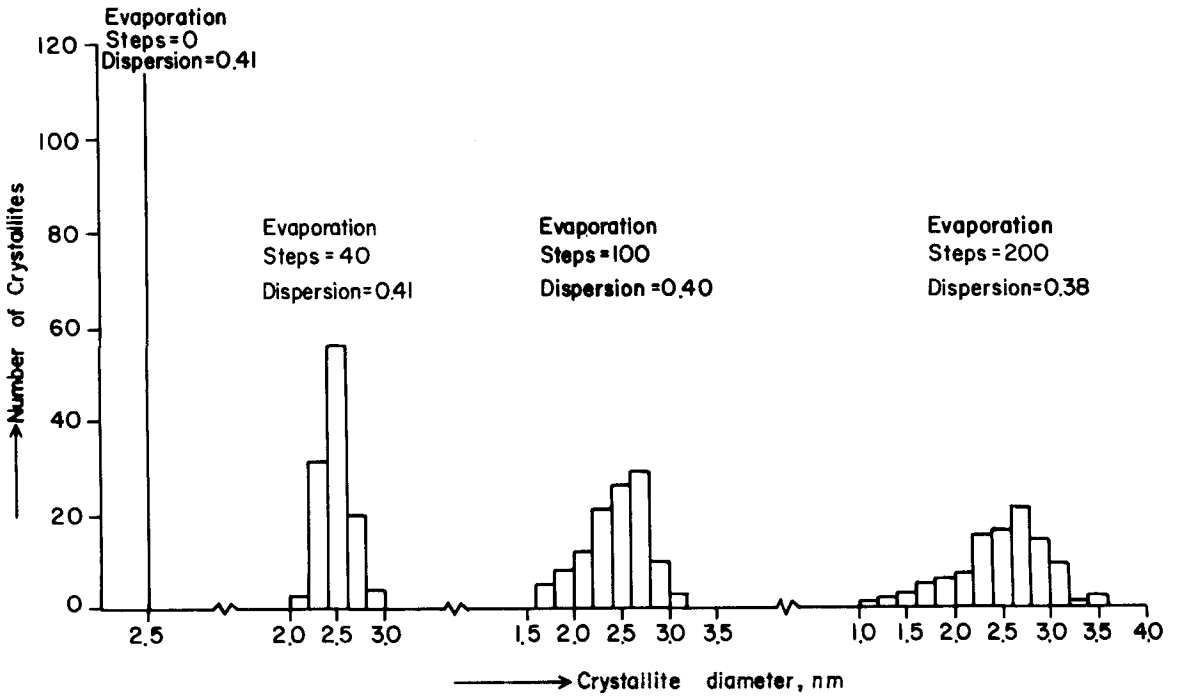

Figure 5. Time evolution of particle-size distribution.

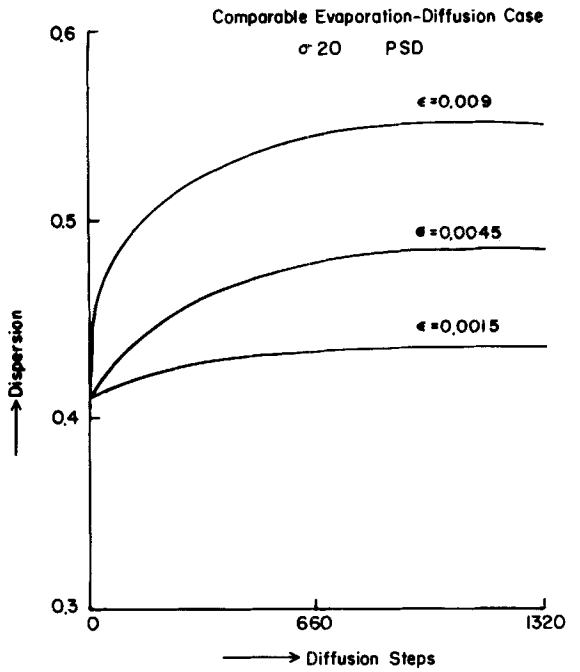

Figure 6. Effect of evaporation rate (comparable evaporation-diffusion mechanism).

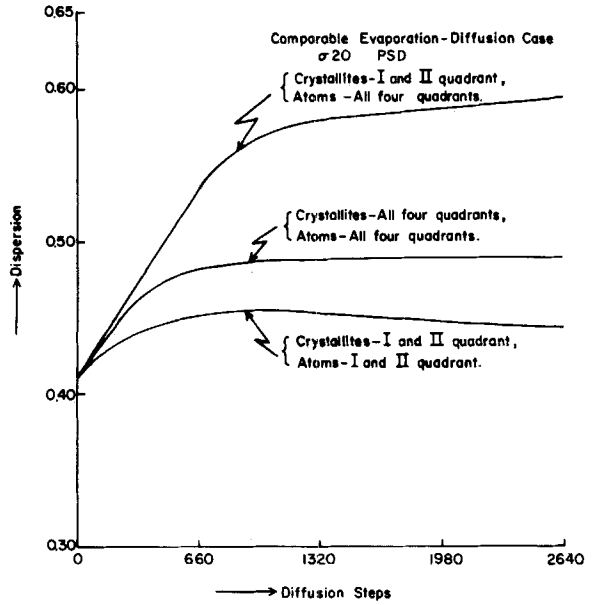

Figure 7. Effect of location of crystallites and atoms on sintering rate.

temperature limit is set by the decomposition of the complex and the lower limit by the slow rate of complex formation.

Fiedirow et al. (1976, 1978) studied the effects on dispersion of oxygen treatments at temperatures up to 873 K for periods of 1 to 128 hours. It was found that exposure to oxygen for one hour resulted in maximum redispersion. Dautzenberg and Walters (1978) found that the increase in dispersion was independent of the length of oxidation exposure (which was varied from 15 minutes to six hours) and the oxygen partial pressure. However, on repeated oxidation-reduction a further increase of the dispersion value was observed. The results indicate that the increase in dispersion on exposure to O_2 may occur very rapidly and suggested a need to study short treatment times.

Catalyst Preparation, Outgassing and Reduction Conditions

The catalyst used was 1.62% Pt on alumina prepared by impregnation of chloroplatinic acid. Hydrogen chemisorption values at 523 K and 32 kPa were selected as representative of monolayer coverage (Spendel and Boudart, 1960). Blank correction for adsorption on the support was made. Reduction was done in flowing H_2 for four hours at 598 K. Outgassing of the catalyst under evacuated conditions ($>1.33 \times 10^{-3}$ Pa) for four hours at 773 K resulted in reproducible adsorption measurements.

TABLE 2. EFFECT OF HYDROGEN AND OXYGEN TREATMENT ON Pt DISPERSION

Run	Treatment (sequential)	Dispersion Experimental	Simulated
1	Fresh Catalyst 1	1.02	1.00
2	Treated in H_2 @ 773 K for 1 hour	0.63	0.63
3	Treated in H_2 @ 773 K for 1 hour	0.55	0.58
4	Treated in O_2/He @ 823 K for 5 min	0.68	0.70
5	Treated in O_2/He @ 823 K for 5 min	0.74	0.72
6	Treated in O_2/He @ 823 K for 5 min	0.79	0.74
7	Treated in O_2/He @ 823 K for 10 min	0.74	0.64
1	Fresh Catalyst 2	0.71	0.71
2	Treated in O_2/He @ 823 K for 5 min	0.69	0.70
3	Treated in O_2/He @ 823 K for 5 min	0.67	0.70
4	Treated in O_2/He @ 823 K for 1 h	0.51	0.49
5	Treated in O_2/He @ 823 K for 5 min	0.51	0.50
6	Treated in H_2 @ 773 K for 1 h	0.41	0.40
7	Treated in O_2/He @ 823 K for 5 min	0.49	0.51
8	Treated in O_2/He @ 823 K for 5 min	0.45	0.52
9	Treated in O_2/He @ 823 K for 5 min	0.48	0.52
10	Treated in O_2/He @ 823 K for 5 min	0.48	0.52
11	Treated in O_2/He @ 823 K for 10 min	0.47	0.47
12	Treated in O_2/He @ 773 K for 5 min	0.47	0.47
13	Treated in O_2/He @ 773 K for 1 h	0.42	0.39
14	Treated in O_2/He @ 823 K for 5 min	0.41	0.42
1	Fresh Catalyst 3	1.08	1.00
2	Treated in O_2/He @ 723 K for 1 h	1.05	1.00
3	Treated in O_2/He @ 823 K for ½ h	0.98	1.00
4	Treated in O_2/He @ 823 K for ½ h	0.95	1.00
5	Treated in O_2/He @ 723 K for 5 min	0.92	1.00
6	Treated in O_2/He @ 823 K for 1 h	0.91	0.99
7	Treated in O_2/He @ 823 K for 1 h	0.90	0.93
8	Treated in O_2/He @ 898 K for ½ h	0.59	0.57
9	Treated in O_2/He @ 723 K for 5 min	0.50	0.56
10	Treated in O_2/He @ 723 K for 5 min	0.55	0.55
11	Treated in O_2/He @ 723 K for 5 min	0.50	0.54
12	Treated in H_2 @ 673 K for 1 h	0.47	0.54
13	Treated in H_2 @ 723 K for 1 h	0.47	0.54

TABLE 3. EFFECT OF HELIUM TREATMENT ON Pt DISPERSION

Run	Treatment	Dispersion Experimental	Simulated
	Catalyst 3		
1	Initial Point	0.47	0.54
2	Treated in He @ 773 K for 5 min	0.46	0.54
3	Treated in He @ 823 K for 1 h	0.46	0.54
4	Treated in He @ 823 K for 12 h	0.36	0.41
	Catalyst 4		
1	Fresh Catalyst	0.82	0.82
2	Treated in He @ 823 K for 12 h	0.66	0.63
3	Treated in He @ 823 K for 8 h	0.55	0.57

Sintering and Redispersion Results

The experiments with catalyst 1 and 2 were designed to show the difference in response to oxygen treatments of a catalyst sintered in oxygen to one sintered in hydrogen, Table 2. The initial dispersion of *catalyst 1* was 1.02 and two hydrogen treatments at 773 K for one hour each lowered the dispersion to 0.55. Subsequent treatments in oxygen at 823 K resulted in dispersion levels as high as 0.79 being achieved. The dispersion value increased, although the increase became progressively smaller, with every five-minute oxygen treatment.

The objective with *catalyst 2* was to obtain ~0.55 dispersion level as with catalyst 1 but to achieve it in O_2 rather than H_2 and then to see if treatments similar to the above would result in redispersion. Run 5, as well as other five-minute O_2 treatments, indicates that O_2-sintered catalysts respond differently to subsequent oxygen treatments than H_2-sintered catalysts.

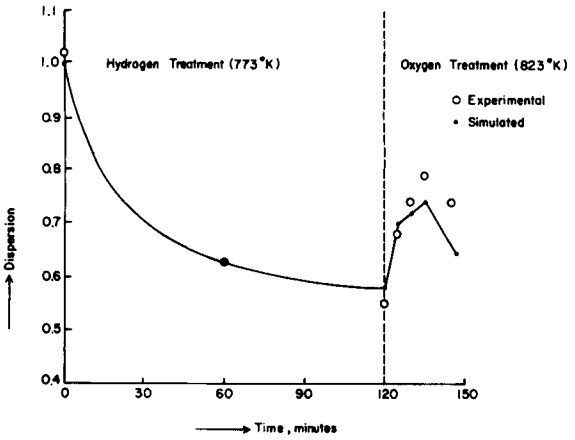

Figure 8. Comparison of experimental and simulated values of Pt dispersion (catalyst 1).

With the dispersion level at 0.51 the catalyst was sintered to 0.41 in H_2. Subsequent treatment in O_2 at 823 K restored the dispersion to 0.49. The catalyst was then sintered in oxygen for one hour to a dispersion level of 0.42. Subsequent treatments in O_2 caused no significant change in the dispersion. It was observed that a dispersion level obtained by O_2 sintering cannot be exceeded by subsequent treatments. Thus no treatment could cause the dispersion level to exceed 0.51.

The purpose of the experimental with *catalyst 3* was to investigate a range of oxygen treatment temperature and times for a catalyst sintered in O_2. The catalyst was found to sinter very slowly in the high dispersion range and no evidence of redispersion was found.

Several experiments were made to compare sintering rates in He with those in O_2 and H_2 atmospheres. As shown in Table 3, in a He atmosphere treatment times of one hour or less at 823 K resulted in no significant change in dispersion. Sintering rates in He were observed to be much slower than in either O_2 and H_2.

COMPARISON OF SIMULATION AND EXPERIMENTAL RESULTS

When in an oxidizing atmosphere evaporation from the crystallites was assumed to be instantaneous with capture and diffusion limiting the rate of sintering. While in a reducing or inert atmosphere it was assumed that very few atoms would be on the support surface at any instant. Diffusion was, therefore, assumed to be instantaneous, capture very rapid and evaporation limiting the rate of sintering.

Catalyst 1. The initial dispersion of this catalyst was 1.0, that is all Pt atoms exposed. Since in H_2 nucleation is taken to be very rapid, it was assumed that the metal atoms formed 1-nm crystallites (dispersion of crystallites ≤ 1 nm was set equal to unity) on subjection to H_2. After evaporation and using the instantaneous diffusion mechanism and a sticking probability of one, a new *PSD* was generated with some crystallites >1 nm and some <1 nm. The crystallites of size <1 nm were assumed to immediately coalesce into a lesser number of 1-nm crystallites. In effect, in a reducing atmosphere it has been assumed that very small crystallites migrate.

Table 2 shows the comparison of simulated and experimental values of dispersion. The one hour H_2 treatments at 773 K correspond to six evaporations in the hour with $\epsilon = 1$.

After the H_2 treatments the system was subjected to O_2. With the *PSD* known, simulation of this condition was done by using the instantaneous evaporation mechanism and the crystallite-size-dependent sticking probability. The five-minute O_2 treatments at 823 K correspond to instantaneous evaporation with $\epsilon = 3$ followed by 165 diffusion steps by the atoms. The 10-minute treatments in O_2 at 823 K were then simulated by using twice the number of diffusion steps with ϵ unchanged. Figure 8 shows that the agreement betweeen experimental and simulated values of dispersion is very reasonable.

Catalyst 2. The initial dispersion of this catalyst was 0.71. Since capture in O_2 is taken to be very slow it was assumed that crystallites originated at only five nucleation sites and the remainder of the atoms were present as free atoms on the surface. Thus the initial *PSD* consisted of five 5-nm crystallites, randomly located on the support and 34,500 free atoms.

The parameters for H_2 at 773 K and for O_2 at 823 K were established with catalyst 1 and were maintained at these values. Namely, for H_2 at 773 K, six evaporations per hour with $\epsilon = 1$, while for O_2 at 823 K, $\epsilon = 3.0$. For O_2 at 773 K, ϵ was reduced from 3.0 to 1.0 and the number of diffusion steps from 165 to 66. Figure 9 and Table 2 show the simulated and experimental results.

After step 5, a 5-minute O_2 treatment, the *PSD* consisted of 5 crystallites of size 5.7, 5.7, 5.9, 6.0 and 6.1 nm and 21,300 free atoms. This was then subjected to H_2 in which the free atoms reverted to 852 1-nm crystallites.

Catalyst 3. The initial dispersion of this catalyst was 1.0. Whereas in H_2 a completely dispersed metal was taken to be in the form of

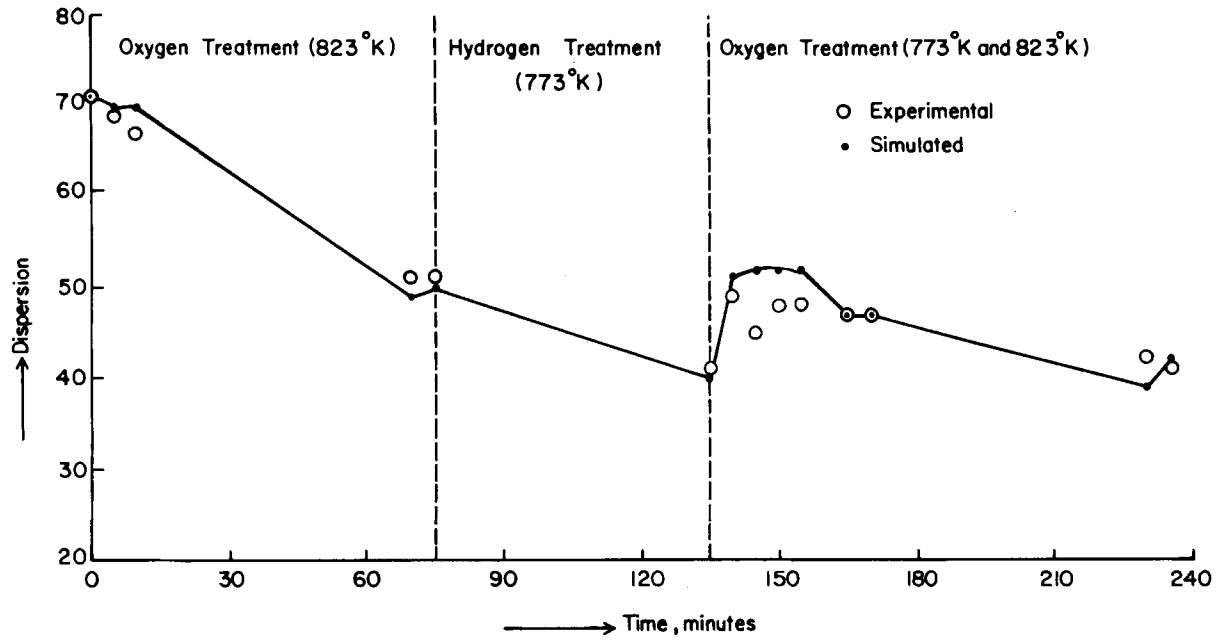

Figure 9. Comparison of experimental and simulated values of Pt dispersion (catalyst 2).

1-nm crystallites, in O_2 the metal was assumed to be present as free atoms on the surface. Nucleation of completely dispersed catalyst in O_2 was simulated by again assuming five nucleation sites, but this time the size was chosen to be 0.277 nm, the diameter of the Pt atom.

At 723 K, $\epsilon = 0$ and there were 33 diffusion steps, while at 898 K these values were 6 and 495, respectively. The simulated and experimental results are shown in Table 2. In hydrogen below 773 K evaporation was assumed to be zero.

Table 3 shows the simulated and experimental results for sintering in an inert atmosphere. The treatments at 823 K correspond to one evaporation per hour with $\epsilon = 0.42$. The assumptions used in the simulation were the same as for a reducing atmosphere.

ACKNOWLEDGMENT

This work was conducted under the sponsorship of the Engineering Experiment Station of Kansas State University.

NOTATION

a = Avogadro number
$(CN)_{corner}$ = coordination number of corner atoms in an FCC crystallite
$(CN)_{face}$ = coordination number of face atoms in an FCC crystallite
$(CN)_{edge}$ = coordination number of edge atoms in an FCC crystallite
D = diameter of crystallite, nm
D_i = a particular crystallite size in a size distribution, nm
D_p = pore diameter, nm
D_s = size of support, nm
d_o = diameter of metal atom, nm
$DISP$ = metal dispersion
DL = step length for diffusion step, nm
ϵ = extent of evaporation
I = number of atoms monitored for Monte Carlo simulations
L = metal loading, %
m = number of atoms along the edge of an fcc crystallite
MW_m = molecular weight of metal, kg/kmol
N = total number of metal atoms in system
n = number of crystallites
N_B = number of bulk atoms in crystallite
N_{corner} = number of corner atoms in crystallite
N_d = number of diffusion steps
N_{face} = number of face atoms in crystallite
N_{edge} = number of edge atoms in crystallite
n_i = number of crystallites of size D_i in a size distribution
N_S = number of surface atoms in crystallite
N_T = number of total atoms in crystallite
S_s = specific surface area of support, m^2/g
SCN = average surface coordination number
V_p = normalized cumulative pore volume, m^3/g
Φ = fraction of surface atoms lost from crystallite

LITERATURE CITED

Baker, R. T. K., C. Thomas, and R. B. Thomas, "Continuous Observation of the Particle Size Behavior of Platinum on Alumina," *J. Catal.*, **38**, 510 (1975).

Baker, R. T. K., E. B. Prestridge, and R. L. Garten, "Electron Microscopy of Supported Metal Particles. I. Behavior of Pt on Titanium Oxide, Aluminum Oxide, Silicon Oxide, and Carbon," *J. Catal.*, **56**, 390 (1979a).

Baker, R. T. K., E. B. Prestridge, and R. L. Garten, "Electron Microscopy of Supported Metal Particles. II: Further Studies of Pt/TiO_2," *J. Catal.*, **59**, 293 (1979b).

Baker, R. T. K., "Effect of Wetting on the Morphology of Supported Platinum Crystallites," *J. Catal.*, **63**, 523 (1980).

Brennan, H. M., H. S. Seelig, and R. W. Van der Haar, "Reactivation of Platinum Catalysts," U.S. 3,117,076 (1964).

Bonzel, H. P., and R. Ku, "On the Kinetics of Oxygen Adsorption of a Pt(111) Surface," *Surf. Sci.*, **40**, 85 (1973).

Chen, M., and L. D. Schmidt, "Morphology and Sintering on Pt Crystallites on Amorphous SiO_2," *J. Catal.*, **55**, 348 (1978).

Coe, R. H., and H. E. Randaltt, "Platinum Group Hydroforming Catalyst Reactivation Process," U.S. 3,278,419 (1966).

Dautzenberg, F. M., and H. B. M. Wolters, "State of Dispersion of Pt in Alumina-Supported Catalysts," *J. Catal.*, **51**, 26 (1978).

deBoer, J. H., "The Dynamical Character of Adsorption," Oxford University Press, London, p. 7 (1968).

Den Otter, G. J., and F. M. Dautzenberg, "Metal-Support Interaction in Pt/Al_2O_3 Catalysts," *J. Catal.*, **53**, 116 (1978).

Dreger, L. H., and J. L. Margrave, "Vapor Pressure of Platinum Metals I. Palladium and Platinum," *J. Phys. Chem.*, **64**, 1323 (1960).

Fiedorow, R. M. J., and S. E. Wanke, "The Sintering of Supported Metal Catalysts. I: Redispersion of Supported Platinum in Oxygen," *J. Catal.*, **43**, 34 (1976).

Fiedorow, R. M. J., B. S. Chahar, and S. E. Wanke, "The Sintering of Supported Metal Catalysts. II. Comparison of Sintering Rates of Supported Pt, Ir and Rh Catalysts in Hydrogen and Oxygen," *J. Catal.*, **51**, 193 (1978).

Flynn, P. C., and S. E. Wanke, "A Model of Supported Metal Catalysts Sintering. I. Development of Model," *J. Catal.*, **34**, 390 (1974a).

Flynn, P. C., and S. E. Wanke, "A Model of Supported Metal Catalyst Sintering. II: Application of Model," *J. Catal.*, **34**, 400 (1974b).

Handa, P. K., "Modeling and Experimental Studies of Sintering and Redispersion of Supported Metal Catalysts," Ph.D. Dissertation, Kansas State University (1981).

Hansen, N., "Evaluation of the Sticking Probability of Gases Chemisorbed on Metal Films Without Measurement of Gas Pressure," *Suppl. Nuovo imento*, **5**, 389 (1967).

Hardeveld, R. V., and F. Hartog, "The Statistics of Surface Atoms and Surface Sites on Metal Catalysts," *Surf. Sci.*, **15**, 189 (1969).

Hayward, D. O., D. A. King, and F. C. Tompkins, "Sticking Probabilities. Heat of Adsorption and Redistribution Processes of N_2 on W Films at 195 and 290° K," *Proc. Roy. Soc., London*, **A297**, 305 (1967).

Kearby, K. K., J. P. Thorn, and J. A. Hinlicky, "Reactivation of Regenerated Noble Metal Catalysts with Gaseous Halogens," U.S. 3,134,732 (1964).

Lee, H. H., "Kinetics of Sintering of Supported Metal Catalysts: The Mechanism of Atom Diffusion," *J. Catal.*, **63**, 129 (1980).

Maat, H. J., and L. Moscou, "A Study of the Influence of Platinum Crystallite Size on the Selectivity of Platinum Reforming Catalysts," *Proc. Int. Congr. Catal.*, 3rd, N. Holland, p. 1277 (1965).

Malo, R. V., I. Munster, and G. M. Webb, "Regeneration of Platinum-Type Hydroforming Catalysts," U.S. 2,879,232 (1959).

McVicker, G. B., R. L. Garten, and R. T. K. Baker, "Surface Area Stabilization of Ir/Al_2O_3 Catalysts by CaO, SrO, and BaO Under Oxygen Atmosphere: Implication on the Mechanism of Catalyst Sintering and Redispersion," *J. Catal.*, **54**, 129 (1978).

Menon, P. G., and G. F. Froment, "Modification of the Properties of $Pt-Al_2O_3$ Catalysts by Hydrogen at High Temperatures," *J. Catal.*, **59**, 138 (1978).

Ruckenstein, E., and B. Pulvermacher, "Kinetics of Crystallite Sintering During Heat Treatment of Supported Metal Catalysts," *AIChE J.*, **19**, 356 (1973a).

Ruckenstein, E., and B. Pulvermacher, "Growth Kinetics and Size Distributions of Supported Metal Crystallites," *J. Catal.*, **29**, 224 (1973b).

Ruckenstein, E., and M. L. Malhotra, "Splitting of Platinum Crystallites Supported on Thin, Nonporous Alumina Films," *J. Catal.*, **41**, 303 (1976).

Ruckenstein, E., and Y. F. Chu, "Redispersion of Platinum Crystallites Supported on Alumina-Role of Wetting," *J. Catal.*, **59**, 109 (1979).

Ruckenstein, E., and D. B. Dadyburjor, "Mechanisms of Aging of Supported Metal Catalysts," *J. Catal.*, **48**, 73 (1977).

Schäfer, V. H., and A. Tebben, "Gleichgewichtsmessungen im System Platin-Sauerstoff. Gasförmiges Platindioxyd," *Z. Anorg. u. Allgem. Chem.*, **304**, 317 (1960).

Spenadel, L., and M. Boudart, "Dispersion of Platinum on Supported Catalysts," *J. Phys. Chem.*, **64**, 204 (1960).

Straguzzi, G. I., H. R. Aduriz, and C. E. Gigola, "Redispersion of Platinum on Alumina Support," *J. Catal.*, **66**, 171 (1980).

Stulga, J. E., P. Wynblatt, and J. K. Tien, "Particle Splitting and Redispersion Phenomena in Model Alumina-Supported Platinum Catalysts,"

J. Catal., **62**, 59 (1980).
Wang, T., and L. D. Schmidt, "Morphology and Redispersion of Ir on SiO_2 in Oxidizing and Reducing Atmospheres," *J. Catal.*, **66**, 301 (1980).
Wanke, S. E., and P. C. Flynn, "The Sintering of Supported Metal Catalysts," *Catal., Rev.*, **12**, 93 (1975).
Webb, G. M., "Rejuvenation of Platinum-Type Hydroforming Catalysts," U.S. 3,011,968 (1961).
Wynblatt, P., and N. A. Gjostein, "Particle Growth in Model Supported Catalysts-I. Theory," *Acta Metallurgica*, **24**, 1165 (1976).
Wynblatt, P., "Particle Growth in Model Supported Metal Catalysts-II. Comparison of Experiment with Theory," *Acta Metallurgica*, **24**, 1175 (1976).
Yao, H. C., M. Sieg, and H. K. Plummer, Jr., "Surface Interactions in the Pt/γ-Al_2O_3 System," *J. Catal.*, **59**, 365 (1979).

Manuscript received March 29, 1982; revision received October 18, and accepted October 28, 1982.

Restrictive Diffusion in Aluminas

The effect of the ratio of solute molecular diameter to the substrate pore diameter on the diffusion of polyaromatic compounds in four different pore sizes of amorphous gamma-aluminas was studied at atmospheric pressure and ambient temperature. Diffusion rates of the polyaromatic compounds in the aluminas decreased as the ratio of solute molecular diameter to pore diameter increased. Empirical correlations between the apparent reduction in solute effective diffusivity and the ratio of molecular diameter to pore diameter were obtained.

A. CHANTONG and F. E. MASSOTH

Department of Fuels Engineering
University of Utah
Salt Lake City, UT 84109

SCOPE

Supported catalysts are normally used in upgrading of coal-derived liquids. Of primary concern is the question of whether the large, multiringed aromatic compounds found in coal-derived liquids will diffuse into the pore structure of the support to reach the active sites at sufficiently rapid rates required for an effective catalyst. When the compound molecular size becomes significant with respect to the pore size, the diffusion rate of the compound in liquid-filled pores becomes less than would be expected from an unrestricted liquid medium. If the diffusion rate of the aromatic compound is the slow step compared to the surface reaction rate, only the outer portion of the catalyst will be utilized. Therefore, knowledge of the effect of the ratio of solute molecular size to pore size on the effective diffusivity of a solute in liquid-filled pores is necessary to utilize the catalyst more effectively.

Studies on membrane diffusion (Renkin, 1954; Beck and Schultz, 1970) have clearly indicated that, by increasing the solute size, the diffusion rate of large solute molecules through certain types of membranes decreases much more rapidly than would be expected from the differences in bulk diffusivity of the solutes alone. This phenomenon has been explained on the basis of reduction of solute mobility resulting from the comparable sizes of the solute and the membrane pores, and has been called restrictive diffusion. Diffusivities of organic solutes in zeolite pores are many orders of magnitude lower than bulk values (Barrer and Brook, 1953; Ruthven and Doetsch, 1976; Satterfield and Cheng, 1972). The lowering in the diffusivities was partially credited to the restrictive effect. Due to the extremely small pore size of zeolites, the ratios of molecular size to pore size were normally greater than 0.8. At these high ratios, it was found that not only the restrictive effect slowed down the pore diffusion rate but adsorbate-adsorbent interaction and type of solvent used also affected the diffusion rate.

Few studies have been done on diffusion of polyaromatic compounds in alumina where ratios of molecular size to pore size are in the same range as those in the membrane diffusion studies. But for diffusion of polyaromatic compounds in alumina, both adsorption and diffusion occur simultaneously in the pores, whereas only diffusion takes place in the pores for the membrane diffusion system. Polyaromatic compounds are expected to be highly adsorbed by alumina. It was found that diffusion within activated carbons of highly adsorbed solutes were dominated by a surface diffusion mechanism (Fritz et al., 1981; Sudo et al., 1978).

In the present work, a systematic sorptive diffusion study of various-sized model compounds in porous alumina particles of different pore sizes was carried out. To simulate the multiringed aromatic compounds in coal-derived liquids and the supports used in the upgrading process, model polyaromatic compounds and activated aluminas were chosen for the sorptive diffusion study. The experiments involved measurement of effective diffusivities of selected polyaromatic compounds (critical molecular diameters 0.7–1.9 nm) in γ-aluminas (pore diameters 4.9–15.4 nm). The major objective was to relate the restrictive effect of pore diffusion on molecular size and alumina pore size. The work also examined a possible surface diffusion contribution.

CONCLUSIONS AND SIGNIFICANCE

Equilibrium adsorption experiments were carried out to determine the type of isotherm which was needed in the mathematical treatment of the kinetic data. Equilibrium adsorption isotherms of all the solutes were nonlinear and were well represented by Freundlich isotherms. The amount of solute uptake by alumina was shown to increase in the order of naphthalene < coronene < octa-ethylporphyrin ≈ tetra-phenylporphyrin for a given alumina.

Effective diffusivities at ambient temperature and pressure were determined by applying a pore diffusion model with a Freundlich isotherm to diffusion run data. The effective dif-

Correspondence concerning this paper should be addressed to F. E. Massoth